Magnetic moment of the $11/2^-$ isomeric state in ^{99}Mo and neutron spin g factor quenching in $A \approx 100$ nuclei

J. M. Daugas,[1,2] B. Rosse,[1] D. L. Balabanski,[3] D. Bucurescu,[4,5] S. Kisyov,[4] P. H. Regan,[6,7] G. Georgiev,[8] L. Gaudefroy,[1,9] K. Gladnishki,[10] V. Méot,[1,9] P. Morel,[1,9] S. Pietri,[11] O. Roig,[1,9] and G. S. Simpson[12]

[1]*CEA, DAM, DIF, 91297 Arpajon, France*
[2]*Université Paris Saclay, CEA, CNRS, Inserm, SHFJ, BioMaps, 91401 Orsay, France*
[3]*Extreme Light Infrastructure - Nuclear Physics (ELI-NP), Horia Hulubei National Institute for R&D in Physics and Nuclear Engineering (IFIN-HH), 077125 Bucharest-Măgurele, Romania*
[4]*Horia Hulubei National Institute for R&D in Physics and Nuclear Engineering (IFIN-HH), 077125 Bucharest- Măgurele, Romania*
[5]*Center for Advanced Studies in Physics of the Romanian Academy, 13, Calea 13 Septembrie, Bucharest, Romania*
[6]*Department of Physics, University of Surrey, Guildford, GU2 7XH, United Kingdom*
[7]*National Physical Laboratory, Teddington, Middlesex TW11 0LW, United Kingdom*
[8]*Université Paris-Saclay, CNRS/IN2P3, IJCLab, 91405 Orsay, France*
[9]*Université Paris Saclay, CEA, Lab Mat Condit Extrêmes, 91680 Bruyères Le Châtel, France*
[10]*Faculty of Physics, St. Kliment Ohridski University of Sofia, 1164 Sofia, Bulgaria*
[11]*GSI Helmholtzzentrum fur Schwerionenforschung GmbH, Planckstr. 1, 64291 Darmstadt, Germany*
[12]*LPSC, CNRS/IN2P3, Université Joseph Fourier Grenoble 1, INPG, 38026 Grenoble Cedex, France*

(Received 1 February 2021; revised 21 July 2021; accepted 2 August 2021; published 13 August 2021)

The gyromagnetic factor of the low-lying $E_x = 684.10(19)$ keV isomeric state of the nucleus ^{99}Mo was measured using the time-dependent perturbed angular distribution technique. This level is assigned a spin and parity of $J^\pi = 11/2^-$, with a half-life of $T_{1/2} = 742(13)$ ns. The state of interest was populated and spin-aligned via a single-neutron transfer on a highly enriched ^{98}Mo target. A magnetic moment $\mu_{\text{expt.}} = -0.627(20)\mu_N$ was obtained. This result is far from the Schmidt value expected for a pure single-particle $\nu h_{11/2}$ state. A comparison of experimental spectroscopic properties of this nucleus is made with results of multishell Interacting boson-fermion Model (IBFM-1) calculations. In this approach, the $J^\pi = 11/2^-$ isomeric state in ^{99}Mo has a pure $\nu h_{11/2}$ configuration. Its magnetic moment, as well as that of other two excited states could be reasonably well reproduced by reducing the free neutron spin g factor with a quenching factor of 0.45. This low value is not appropriate only for this case, similar values for the quenching factor being also required in order to describe magnetic moments in other nuclei from the same mass region.

DOI: 10.1103/PhysRevC.104.024321

I. INTRODUCTION

The nuclear magnetic-dipole moment is a highly sensitive probe of the single-particle properties of the nuclear wave function. The gyromagnetic factor (g factor) of a state is the ratio of its magnetic moment μ to spin J, $g = \mu/J$. The knowledge of the g factor of a state can allow confirmations of spin and parity assignments and provide information on the valence-orbit occupancy. Because magnetic moments only depend on the wave function of the studied nuclear state and not on the transition between states as for transition probabilities or spectroscopic factors, their knowledge is a good test for the wave functions of different nuclear models. It has been shown recently that the magnetic moments of states in odd-mass nuclei are also sensitive to the nature of the collective excitations (particle-vibration or particle-rotor model) [1].

Magnetic moments for the neutron $h_{11/2}$ orbital at the closed proton $Z = 50$ shell [2] display a smooth variation along the Sn isotopes with an extracted g factor around $g = -0.25$. This result is in perfect agreement with the effective Schmidt value [3] applying a common quenching factor of 0.7 to the free single-particle g factor of the spin motion, $g_s^{\text{eff}} = 0.7 g_s^{\text{free}}$, reflecting the effect of the core polarization and the meson exchange current. Measurements of the g factors for the same orbital below the $Z = 50$ shell have been made for many isotopes along the Cd, $Z = 48$, chain, above the neutron number $N = 59$ [2,4]. Experimental values are still displaying a smooth variation. For both cases, the smooth variation of the occupation numbers has been attributed to strong pairing correlations [5]. The g factors for the Cd isotopes are found to be about 25% below the Sn ones, around $g = -0.20$. Here, one has to reduce the quenching factor down to 0.6 to reproduce the measured g factors. It is interesting to note that the same feature was observed by reproducing the experimentally reduced transition probability $B(M2)$ values between the $\nu h_{11/2}$ and $\nu g_{7/2}$ configurations in $^{95-99}$Mo, ^{99}Ru, and ^{101}Pd which were satisfactorily described within the quasiparticle-phonon model using $g_s^{\text{eff}} = 0.6 g_s^{\text{free}}$ [6]. Thus, the importance

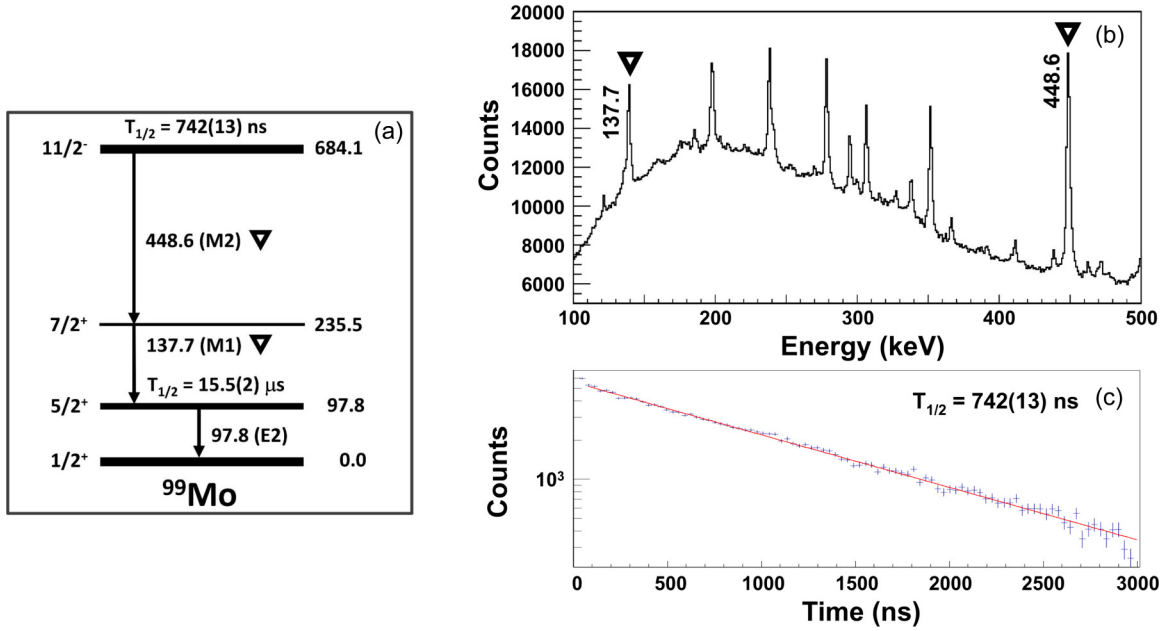

FIG. 1. (a) The decay scheme of the $11/2^-$ isomer in ^{99}Mo. (b) Typical delayed γ-ray spectrum from the ^{98}Mo(d, p) ^{99}Mo reaction at 6 MeV. Observed isomeric transitions are labeled with open triangles. (c) Time spectrum of the 448.6 keV transition.

of the core polarization depends on the filling of the proton shell.

Farther away from $Z = 50$ only one g factor has been measured so far for the $J^\pi = 11/2^-$ state in the ^{103}Pd isotope with $Z = 46$ and $N = 57$, where a value of $g = -0.19(1)$ [2] was reported. The uncertainty of this result does not allow us to judge the evolution of the g factor when going from two to four proton holes away from a closed shell. Therefore, it is important to investigate the g factor of the $\nu h_{11/2}$ orbital for isotopes below Cd and Pd in order to get information on the evolution of the wave function, of the quenching factor, and the role of the core polarization when going away from closed proton shell.

The $Z = 42$ molybdenum isotopes, with mass number around 100, lie in a transitional region where different degrees of freedom influence the evolution of nuclear structure. The work of Regan and collaborators [7] reveals the interplay between rotational motion and vibrations in the Mo nuclei. The $\nu h_{11/2}$ intruder orbital defines the collective properties in this mass region. Regular sequences of γ rays which are built on the $\nu h_{11/2}$ orbital have been observed throughout the region [8–13]. In ^{99}Mo, a second microsecond isomeric level, located above the $T_{1/2} = 15.5$ μs, $J^\pi = 5/2^+$, $E_x = 97.785$ keV one [14], at an excitation energy of $E_x = 684.10$ keV was first observed by the work of Ref. [15]. This second isomeric state will be noted in the following as ^{99m2}Mo. A spin and parity assignment was reported to be $J^\pi = 11/2^-$ [15,16], with an expected pure $\nu h_{11/2}$ configuration. The ^{99m2}Mo state has a weakly prolate shape and was identified as the head of the decoupled band associated with the population of the low-K components of the unique-parity $\nu h_{11/2}$ orbital [10,16]. The level scheme and decay path of the two isomers are presented in Fig. 1(a). ^{99m2}Mo decays via the 448.6 keV $M2$ transition to the $J^\pi = 7/2^+$ level with a mainly $\nu g_{7/2}$ configuration with a reduced transition rate of $B(M2) = 0.103(8)$ Weisskopf units (W.u.) [17]. Furthermore, the γ decay proceeds via a relatively prompt 137.7 keV $M1$ transition to the first isomeric state [18].

To gather more spectroscopic information on the $11/2^-$ isomeric state and on the evolution of the quenching factor, the g factor of this isomeric state has been measured; results and interpretations are presented in the following.

II. EXPERIMENTAL MEASUREMENTS

The experiment was performed at the tandem accelerator of the CEA Bruyères le Châtel, France. The ^{99}Mo isotope was produced in different excited states [19] and spin-aligned [20] in a (d, p) reaction with a pulsed 6 MeV energy deuteron beam impinging on a highly enriched annealed ^{98}Mo target. At the same time the target was used as a nonperturbative host. The $l = 5$ transitions were found to be strong [21], allowing sufficient production rate of the $J^\pi = 11/2^-$ state to be investigated. The spin-oriented ensemble of an isomeric state induces anisotropy in the γ-ray emission. The time-dependent perturbed angular distribution (TDPAD) method was applied for the measurement of this anisotropy, leading to the g factor determination of the metastable state ^{99m2}Mo, $E_x = 684.10$ keV and $J^\pi = 11/2^-$.

The TDPAD apparatus consisted of a single-crystal host, namely, the ^{98}Mo target, a dipole electromagnet, and γ-ray detectors. Under an external magnetic field B_0 perpendicular to the beam axis which corresponds to the spin-orientation axis, the spin precesses the ensemble with a Larmor frequency $\omega_L = -g\mu_N B_0/\hbar$, where g is the g factor, μ_N the nuclear magneton, and $\hbar$ the reduced Planck constant. The observation of the γ-ray anisotropy synchronized with the Larmor precession enables us to determine the g factor.

Data acquisition was done in an event-by-event mode within a 3 μs time range that was triggered by the γ radiation and stopped by the radio-frequency signal of the pulsation of the tandem. The γ rays were observed with four high-purity germanium detectors (HPGe) positioned in the horizontal plane at $\pm 135^\circ$ and $\pm 45^\circ$ with respect to the beam axis. Time spectra of each detector were collected, having as $T = 0$ the signal due to the prompt γ ray peak, and as delayed T the γ rays coming from the isomeric decay. The prompt γ ray induces a peak of about 100 ns width. The beam intensity was controlled to avoid stopping of the acquisition by a forthcoming prompt γ ray which might imply random coincidences [22]. The worse timing resolution of the HPGe detectors for γ-ray energies below 150 keV prompted us to only consider the isomeric transition $E_\gamma = 448.6$ keV for the determination of the g factor.

Angular distribution of the γ-ray anisotropy was evaluated with the standard $R(t)$ function giving the difference in the intensities between two detectors positioned at 90° with respect to each other as

$$R(t) = \frac{I(t,\theta) - I(t,\pi/2+\theta)}{I(t,\theta) + I(t,\pi/2+\theta)}, \quad (1)$$

where $I(t,\theta)$ is the γ-ray intensity at time t for the detector positioned at an angle θ. The $R(t)$ function allows us to extract the Larmor frequency as

$$R(t) = \frac{3A_2B_2}{4 + A_2B_2} \cos\left[2(\theta - \omega_L t)\right], \quad (2)$$

where A_2 is the second-order angular distribution coefficient which depends on the multipolarity of the observed γ transition and B_2 is the rank-two orientation tensor which depends on the spin orientation of the emitting state. Here, higher-order terms are neglected.

To include systematic errors, mainly due to the distribution of the magnetic field over the beam spot, we have measured the Larmor precession under identical conditions for the ^{66}Cu isotope, using as target an annealed copper host. The $R(t)$ function of the $J^\pi = 6^-$ isomer having a known g factor of $g = +0.173(2)$ [23] has been done and $B_0 = 0.630(12)$ T was extracted for the applied magnetic field. Both crystals have nonperturbative cubic structures, namely centered face cubic for Cu and centered cubic for Mo. The deduced magnetic field measured by Cu in Cu is assumed to be similar within the error bars of Mo in Mo.

A typical delayed energy spectrum for the ^{98}Mo$(d,p)^{99}$Mo reaction is presented in Fig. 1(b), where the isomeric transitions are clearly observed. The extracted half-life $T_{1/2} = 742(13)$ ns, shown in Fig. 1(c), is in good agreement with previous measurements [15,17] leading to a more precise reduced transition probability $B(M2) = 0.104(3)$ W.u. value. Figure 2 represents the evaluated $R(t)$ function with a 32 ns binning. Assuming a pure $M2$ transition for the $E = 448.6$ keV γ ray, an amount of spin alignment of the order of 15% is deduced. The attenuation of the amplitude of the $R(t)$ function is due to the peak-to-background evolution from β-γ decay and random γ contributions into the energy gate of the isomeric transition. The g factor of ^{99m2}Mo is determined

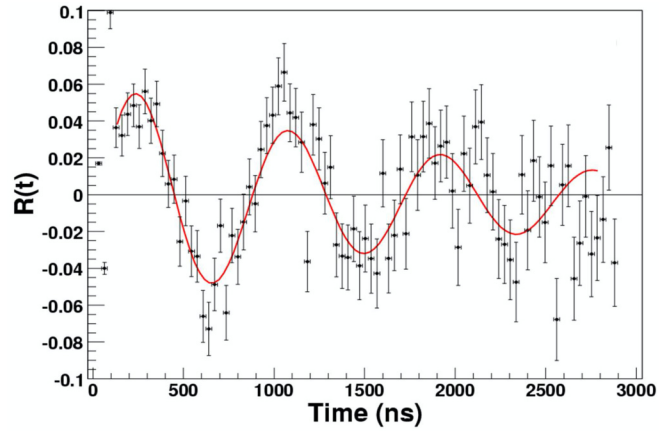

FIG. 2. $R(t)$ function associated with the 448.6 keV delayed γ ray.

to be $g_{\text{expt.}} = -0.114(3)_{\text{stat.}}(2)_{\text{syst.}}$. Thus, knowing the spin of this isomeric state to be $J = 11/2$, its magnetic moment is calculated to be $\mu_{\text{expt.}} = -0.627(20)\mu_N$. This result is far from the magnetic moments observed in the Cd chain and in ^{103}Pd. To obtain a deeper insight into the structure of this state, theoretical calculations were performed in the framework of an algebraic collective model as described in the following.

III. DISCUSSION AND INTERPRETATION

The even-even Mo isotopes around $N \approx 58$ exhibit a shape coexistence phenomenon (see, e.g., Refs. [24–26]), i.e., the occurrence of two configurations (structures) with different shapes. This situation is understood microscopically by the competition between the normal $2p$-$0h$ configuration that shows a vibrational structure, and an "intruder" $4p$-$2h$ configuration, corresponding to proton excitation across the $Z = 40$ subshell closure, showing a deformed character [24]. The mixing of the two configurations into the low-spin states varies with the number of neutrons. Close to $N = 50$ the normal configuration dominates in the ground-state regime, the nuclei showing a vibrational character, and after $N = 60$ the intruder configuration is the lowest and the nuclei become deformed. In between, for $N = 56$ and 58, the mixing is the strongest. Such a situation was described within the interacting boson model (IBM) [27] by mixing two configurations with boson numbers differing by two (IBM-CM) [28]. This model was applied to the Mo isotopes with N from 54 to 62 in Ref. [26], showing that the two configurations cross in energy between the neutron numbers 56 and 58, where the low-lying states have a spherical (deformed) mixing with percentages of about 60% (40%) for $N = 56$ and 38% (62%) for $N = 58$.

The normal extension of the IBM to odd-mass nuclei is the interacting boson-fermion model (IBFM) [29,30], where the nuclei are described by coupling the odd particle to an even-even core described by the IBM. For ^{99}Mo, the core nucleus may be chosen as one of the two neighboring even-even nuclei ^{98}Mo or ^{100}Mo that should be described by the IBM-CM. The presently available IBFM codes, however, do not contain yet

an option for such a core nucleus. We decided, nevertheless, to study the ^{99}Mo nucleus within the IBFM-1 model, which does not distinguish between neutrons and protons, and considers a core described by IBM-1. To this end, we chose as a core ^{100}Mo which, as discussed above, has a low-energy regime dominated by the deformed configuration that has a moderate quadrupole deformation $\beta_2 = 0.234$ [31]. Up to about 2.5 MeV excitation [32], its structure (the quasi-ground and quasi-gamma bands) comprises mostly states originating from the deformed configuration [26]; exception are the low-lying 0_2^+ (695 keV) and 2_3^+ (1492 keV) states, which originate from the spherical configuration. For our IBFM-1 calculations, ^{100}Mo was described with IBM-1 [27], which provided a good description of its ground and quasi-gamma bands. In studying the ^{99}Mo nucleus within IBFM-1 with this core, we hoped that many characteristics of the low-lying states will be reasonably well understood, but one should be aware of the fact that the neglect of the influence of the spherical states may cause a worse agreement for certain states. Thus, the comparison between experimental data and those calculated with the IBFM-1 should be considered with caution.

A. IBFM-1 calculations

The available ODDA, PBEM, and SPEC programs [33], were used to calculate the energy levels, electromagnetic transition rates and moments, and one-neutron transfer spectroscopic factors, respectively. The details of the calculations are similar with those for its neighbor isotope ^{97}Mo [9], where, however, the ^{96}Mo core had a g.s. quasivibrational configuration that was much less mixed with the deformed one. The odd fermion was allowed to occupy the single-particle orbits from the 50 to 82 major shell, namely, $d_{5/2}$, $g_{7/2}$, $s_{1/2}$, $d_{3/2}$, and $h_{11/2}$. For the single-particle (s.p.) energies of these orbitals we started from the values of Ref. [34] and finally chose the values relative to $d_{5/2}$ of 2.4 MeV ($g_{7/2}$), 1.1 MeV ($s_{1/2}$), 3.0 MeV ($d_{3/2}$), and 2.7 MeV ($h_{11/2}$), respectively, which describe well the energies of the lowest states in this nucleus. The strengths of the boson-fermion interaction are $A_0 = -0.05$ MeV, $\Gamma_0 = 0.34$ MeV, and $\Lambda_0 = 1.30$ MeV^2 for the monopole, quadrupole, and exchange interactions, respectively [33]. Both the positive- and negative-parity states were calculated with this Hamiltonian. The calculated negative-parity levels are entirely due to the $h_{11/2}$ orbital.

Figure 3 shows a comparison of the experimental low-energy-level scheme with positive-parity states up to about 1 MeV, and negative-parity states up to about 2 MeV [18], with the results of these calculations. The positive-parity experimental levels are labeled with the level number of the assigned calculated partner. The correspondence between the calculated and experimental levels was based on all known spectroscopic properties: energy levels and their electromagnetic decay mode (branching ratios, known B values) [18], spectroscopic factors for one-neutron pickup (p, d) and (d, t) reactions [35], and magnetic moments (see Ref. [18] and the present measurement).

For the positive-parity states the agreement is reasonable, one may state that most low-spin levels up to $E_x \approx 0.7$ MeV originate mainly from the coupling of the odd-particle to

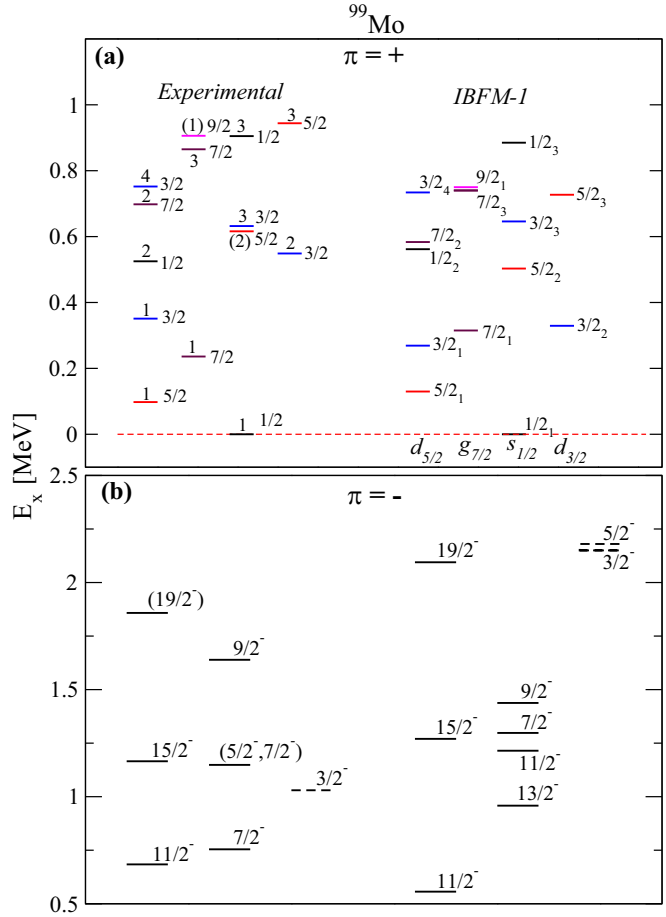

FIG. 3. Comparison between experimental levels and IBFM-1 calculated ones. The IBFM levels are arranged according to their dominant single-particle component of the wave-function. The experimental energy levels are labeled with the order number of the assigned calculated state of the same spin. See also discussion in the text. Experimental levels are from Ref. [18]

the moderately deformed configuration of the core. There are some discrepancies for the B values [the $B(E2)$ of the $5/2_1^+$ state is overestimated by a factor of ten, and the $B(M1)$ of the $7/2_1^+$ state is underestimated], which may indicate the necessity of including the mixing of configurations in the core description. A good description of the known magnetic moments was achieved with a neutron spin g factor $GS = -1.721\mu_N$ (see discussion below), with the following experimental [calculated] values (in μ_N): for the $1/2_1^+$ state, $\pm 0.375(3)$ [-0.719]; for the $5/2_1^+$ state, $-0.775(5)$ [-0.769]; for the $11/2^-$ state, $-0.627(16)$ [-0.626].

For the negative-parity states, the favored $11/2^-$, $15/2^-$, $19/2^-$ sequence is reasonably well reproduced, although with a slightly smaller moment of inertia than the experimental one. The lowest spin members of the calculated multiplet $2^+_{1,\mathrm{core}} \times h_{11/2}$, $7/2^-$ and $9/2^-$, may correspond to known experimental states. The experimental low-lying $3/2^-$ and eventually $(5/2^-)$ states are not accounted for by the calculations because the first calculated states with these spin values are rather high in energy.

B. Magnetic moments and *g*-factor quenching

The $M1$ transition operator contains, in its simplest form [33] used in our calculations, three effective g factors: the d-boson g factor (GD) and the single-particle angular-momentum and spin effective g factors (GL and GS, respectively). A GD value of $0.47\mu_N$ was determined from the g factor of the 2_1^+ state of the core [32]. Since the odd fermion is a neutron, $GL = 0$, while GS is determined from the experimental data. For a free neutron, $GS = -3.826\mu_N$. However, in theoretical calculations it was found that one must use an effective GS value smaller than the free value. In most IBFM calculations a quenching factor of 0.7 was used ($GS = -2.678\mu_N$). By using this customary value the calculated magnetic moment of the $11/2^-$ state was $-1.2\mu_N$, almost the double of the measured $-0.627\mu_N$.

This large difference was first attributed to the possibility that the $11/2^-$ level is not a pure $\nu h_{11/2}$ state. There were two possibilities. (i) The contribution of other negative-parity orbitals in the calculation of the negative-parity states. To test this, we have included the $f_{7/2}$ and $h_{9/2}$ orbitals from the next major shell, above the $N = 82$ gap. Because these orbitals are rather distant, their influence was very small, resulting in a few-percent contribution in the wave function and very small changes of the magnetic moment of the $11/2^-$ state. (ii) The $11/2^-$ state has, besides the single-particle $h_{11/2}$ dominant configuration, some components resulting either from coupling the positive-parity orbitals $d_{5/2}$ or $g_{7/2}$ to the 1.908 MeV, 3^- state of the core, or from couplings of the four positive-parity orbitals to the 4^-, 5^- states resulting from proton excitations like $(p_{1/2}^{-1}g_{9/2}^{1})$. However, both these cases are not energetically favored, therefore their contributions are not expected to be large.

The only possibility to improve the description of the magnetic moment within the present IBFM-1 approach, in which the $11/2^-$ has a pure $h_{11/2}$ single-particle character, was to change the quenching of the free neutron spin g factor. It was found that the magnetic moments are very sensitive to this quantity and that, for a quenching of 0.45 ($GS = -1.721\mu_N$), one can match exactly the experimental magnetic moment of the $11/2^-$ state. This is more than a simple "normalization" (fit of one experimental value) because a similar improvement was *simultaneously* obtained for the magnetic moment of the $5/2_1^+$ state, and some improvement was also obtained for the magnetic moment of the $1/2^+$ ground state, where with the customary quenching of 0.70 the calculated values were around $-1.2\mu_N$ for both these states.

This result prompted us to investigate the value of the quenching factor for other nuclei in the mass ≈100 region. We did this for the following nuclei for which similar IBFM-1 approaches were published, within the same 50–82 shell space: ^{99}Zr [36,38], ^{97}Mo [9], the Ru isotopes 99 to 105 [39], and ^{113}Cd [40]. Similar to the case of ^{99}Mo, the magnetic moments were found to be rather sensitive to the value of the quenching factor, while the $M1$ transition rates were generally less sensitive.

For all these nuclei the published IBFM-1 calculations were made with the usual prescription of 0.7 for the quenching factor, which provided a qualitative agreement with the experimental values (although sometimes magnetic moments were not considered). Figure 4 displays a synthesis of experimental magnetic moments for states of different spins in these nuclei compared with IBFM-1 calculated values for quenching factors of GS between 0.70 and 0.45. One can see that out of eighteen experimental magnetic moments fourteen are best described for quenching factors in the range 0.45 to 0.55. In the case of ^{99}Zr, where one can see that a compromise value of the quenching factor of ≈0.5 provides an optimum description of all three known magnetic moments, it was checked that the $M1$ transition rates were rather insensitive to the variation of GS and thus the conclusions of Refs. [36,38] do not change. One should note the similarity (in magnitude and sign) of the IBFM description of the magnetic moments of five states in ^{113}Cd [Figs. 4(n) to 4(r)] with that provided by a particle-rotor model based on the Nilsson potential for a small deformation of the core [1]. This shows that both these models are able to produce the orbital mixings needed to explain the magnetic moments.

In conclusion, for odd-neutron nuclei in the mass $A \approx 100$ region, IBFM-1 calculations with the odd nucleon occupying the orbitals from the 50 to 82 shell, and a quenching of the free neutron spin g factor of about 0.5, offer the best description of the experimental data, in particular of the magnetic moments which are rather sensitive to this quantity. One should remark that adjusting the quenching factor improves the agreement between the (IBFM) calculations and experiment, but, unfortunately, it does not give an insight into the nuclear structure causing the quenching.

Effective values for the neutron spin g factor, therefore the use of a quenching factor, are also common to other theoretical model approaches, including the shell model. The main reason of this quenching is the inadequacy of the lowest-order shell-model wave functions [41]. Calculations of the core-polarization and meson-exchange current effects lead to equivalent effective one-body $M1$ operators [41]. The completeness of the shell-model space used, as well as its associated effective interaction determine the effective operator, therefore the quenching of the free nucleon g factor. Thus, in calculations for the sd shell [42] and fp shell [43] nuclei, the use of the free-nucleon g factors provided a good description of the experimental data. In contrast, in the f_5pg_9 shell, corresponding to nuclei between ^{57}Ni and ^{96}Pd, a good description of the magnetic moments definitely required a quenching factor of 0.7, which reflects the incompleteness of the model space with respect to the spin-orbit partners; that is, the ^{56}Ni core is not LS closed [44,45].

Large-scale shell-model calculations for ^{111}Cd provided a good description of both signs and magnitudes of experimental magnetic moments for six states using a standard quenching factor of 0.7 [46]. It is interesting that Refs. [1,46] suggest that the good agreement between the particle-rotor and the shell-model descriptions for g factors in Cd isotopes is a result of the fact that the Nilsson wave functions at small deformation provide a good approximation of the shell model, as observed by Lawson [47].

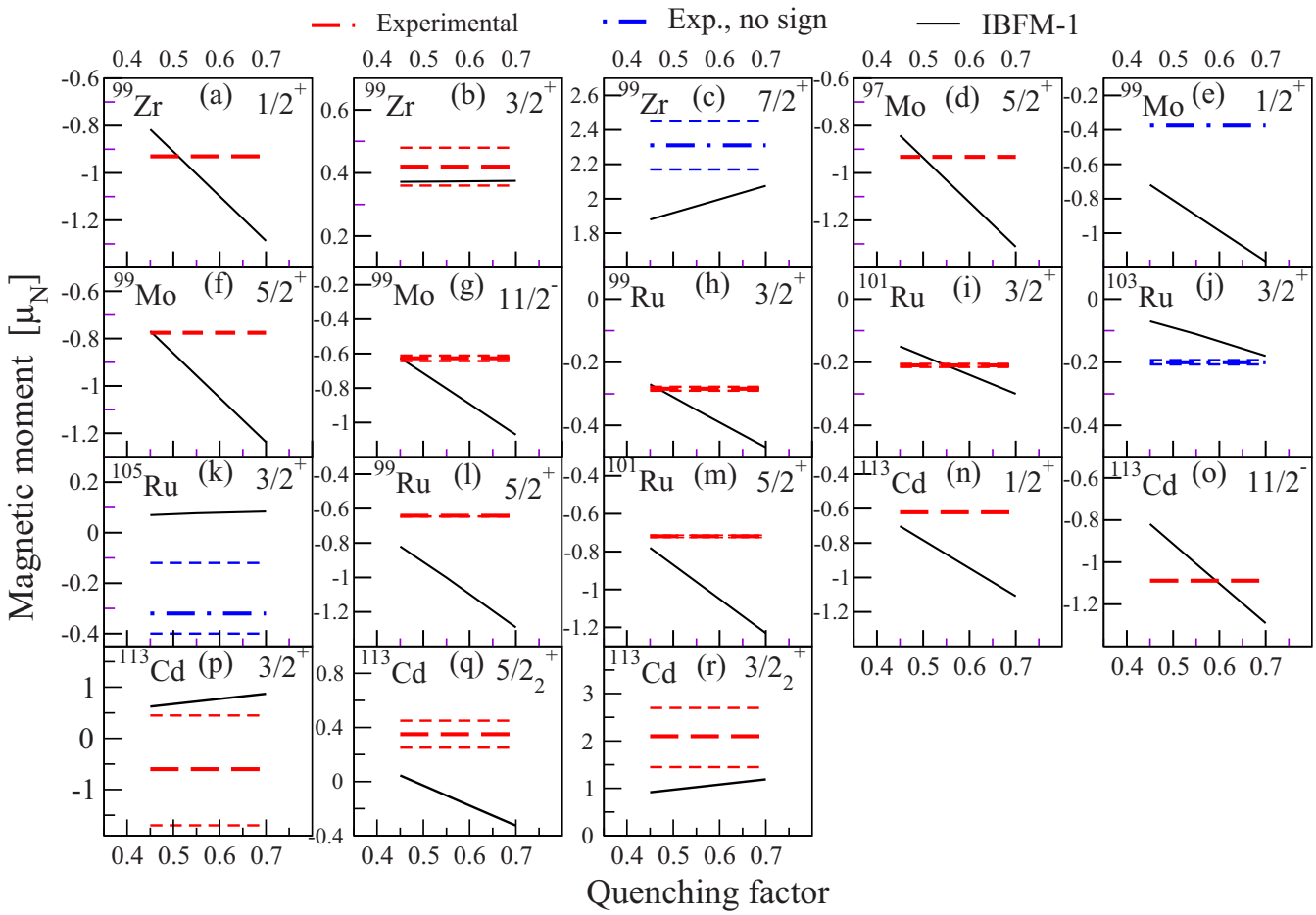

FIG. 4. Comparison between experimental magnetic moments and IBFM-1 values calculated for different quenching factors for the neutron spin g factor. The experimental values are represented by horizontal lines: thick dashed (red) for the values determined with sign, thick dash-dotted (blue) for those determined without sign, and thin dashed lines for the limits of the error bars. The calculated values are the black continuous lines. The experimental values were taken from Ref. [36] (^{99}Zr), Ref. [1] (^{113}Cd), and Refs. [2,37] (for the rest of the nuclei) and refer to ground states and first-excited states with the given spin values, except for ^{113}Cd which include also the second-excited states with $J^\pi = 3/2^+$ and $5/2^+$ [graphs (q) and (r)]. See text for the articles with IBFM-1 approaches of the nuclei from this figure.

IV. CONCLUSIONS

The $11/2^-$ isomeric state of ^{99}Mo was carefully investigated via a g-factor measurement. The measured magnetic moment $\mu_{\text{expt.}} = -0.627(20)\mu_N$ is rather far from the value expected for a pure single-particle $\nu h_{11/2}$ configuration. To shed light on the configuration of this isomeric state, multi-shell IBFM-1 calculations were performed with a ^{100}Mo core and the odd fermion allowed us to occupy the orbitals from the $N = 50$ to 82 shell, although this approach is rather simplistic in view of the shape coexistence phenomenon present in this mass region.

Experimental g factors of three states in this nucleus, including that of the pure $\nu h_{11/2} 11/2^-$ state, were reasonably well reproduced by using a quenching factor of 0.45 for the free neutron spin g factor. The need of such a low value of the quenching factor was confirmed by examining a set of nuclei from the $A \approx 100$ region for which IBFM-1 parametrizations in the same shell orbit space were available. Most of the known magnetic moments in these nuclei clearly asked for a quenching of the free neutron spin g factor of about 0.5. It would be interesting to investigate this quenching in the same nuclei for shell-model calculations with different truncation schemes. The large-scale shell-model calculations for ^{111}Cd [46] represent a move in this direction.

ACKNOWLEDGMENTS

We are grateful to G. Alloy, J. J. Baldys, F. Goffard, and M. Reverberi for providing us the beam. We would like to thank F. Garrido from IJClab for annealing the enriched isotope target.

[1] A. E. Stuchbery, S. K. Chamoli, and T. Kibedi, Phys. Rev. C **93**, 031302(R) (2016).

[2] N. J. Stone, IAEA, International Nuclear Data Committee, INDC(NDS)-0794 (2019); INDC(NDS)-0816 (2020).

[3] T. Schmidt, Z. Phys. **106**, 358 (1937).

[4] D. T. Yordanov, D. L. Balabanski, J. Bieron, M. L. Bissell, K. Blaum, I. Budincevic, S. Fritzsche, N. Frommgen, G. Georgiev, Ch. Geppert, M. Hammen, M. Kowalska, K. Kreim, A. Krieger, R. Neugart, W. Nortershauser, J. Papuga, and S. Schmidt, Phys. Rev. Lett. **110**, 192501 (2013).

[5] D. Riegel, N. Brauer, F. Dimmling, B. Focke, and K. Nishiyama, Phys. Lett. B **46**, 170 (1973).

[6] L. G. Kostova, W. Andrejtseheff, L. K. Kostov, L. Funke, E. Will, and A. I. Vdovin, Z. Phys. A: Hadrons Nucl. **342**, 145 (1992).

[7] P. H. Regan, C. W. Beausang, N. V. Zamfir, R. F. Casten, J.-Y. Zhang, A. D. Yamamoto, M. A. Caprio, G. Gurdal, A. A. Hecht, C. Hutter, R. Krucken, S. D. Langdown, D. A. Meyer, and J. J. Ressler, Phys. Rev. Lett. **90**, 152502 (2003).

[8] Y. H. Zhang, M. Hasegawa, W. T. Guo, M. L. Liu, X. H. Zhou, G. de Angelis, T. M. Axiotis, A. Gadea, N. Marginean, Martinez, D. R. Napoli, C. Rusu, Zs. Podolyak, C. Ur, D. Bazzacco, F. Brandolini, S. Lunardi, S. M. Lenzi, R. Menegazzo, R. Schwengner, A. Gargano, W. von Oertzen, and S. Tazaki, Phys. Rev. C **79**, 044316 (2009).

[9] D. Bucurescu, G. Căta-Danil, I. Căta-Danil, M. Ivaşcu, N. Mărginean, and C. A. Ur, Phys. Rev. C **63**, 014306 (2000).

[10] P. H. Regan, A. D. Yamamoto, F. R. Xu, C. Y. Wu, A. O. Macchiavelli, D. Cline, J. F. Smith, S. J. Freeman, J. J. Valiente-Dobon, K. Andgren, R. S. Chakrawarthy, M. Cromaz, P. Fallon, W. Gelletly, A. Gorgen, A. Hayes, H. Hua, S. D. Langdown, I. Y. Lee, C. J. Pearson *et al.*, Phys. Rev. C **68**, 044313 (2003).

[11] J. Timar, J. Gizon, A. Gizon, D. Sohler, B. M. Nyako, L. Zolnai, A. J. Boston, D. T. Joss, E. S. Paul, A. T. Semple, C. M. Parry, and I. Ragnarsson, Phys. Rev. C **62**, 044317 (2000).

[12] A. D. Yamamoto, P. H. Regan, C. W. Beausang, F. R. Xu, M. A. Caprio, R. F. Casten, G. Gurdal, A. A. Hecht, C. Hutter, R. Krucken, S. D. Langdown, D. Meyer, J. J. Ressler, and N. V. Zamfir, Phys. Rev. C **66**, 024302 (2002).

[13] N. Fotiades, J. A. Cizewski, D. P. McNabb, K. Y. Ding, D. E. Archer, J. A. Becker, L. A. Bernstein, K. Hauschild, W. Younes, R. M. Clark, P. Fallon, I. Y. Lee, A. O. Macchiavelli, and R. W. MacLeod, Phys. Rev. C **58**, 1997 (1998).

[14] R. B. Duffield and S. H. Vegors, Jr., Phys. Rev. **112**, 1958 (1958).

[15] W. Dietrich, G. C. Madueme, L. Westerberg, and A. Backlin, Phys. Scr. **12**, 271 (1975).

[16] J. Dubuc, G. Kajrys, P. Lariviere, S. Pilotte, W. Del Bianco, and S. Monaro, Phys. Rev. C **37**, 954 (1988).

[17] H. Bartsch, K. Huber, U. Kneissl, and H. Krieger, Z. Phys. A: At. Nucl. **285**, 273 (1978).

[18] E. Browne and J. K. Tuli, Nucl. Data Sheets **145**, 25 (2017).

[19] J. B. Moorhead and R. A. Moyer, Phys. Rev. **184**, 1205 (1969).

[20] T. V. Ragland, R. J. Mitchell, R. P. Scharenberg, R. E. Holland, and F. J. Lynch, Phys. Rev. C **18**, 2494 (1978).

[21] W. Booth, S. M. Dalgliesh, K. C. McLean, R. N. Glover, and F. R. Hudson, Phys. Lett. B **30**, 335 (1969).

[22] I. Matea, G. Georgiev, J. M. Daugas, M. Hass, G. Neyens, R. Astabatyan, L. T. Baby, D. L. Balabanski, G. Belier, D. Borremans, G. Goldring, H. Goutte, P. Himpe, M. Lewitowicz, S. Lukyanov, V. Meot, F. de Oliveira Santos, Yu. E. Penionzhkevich, O. Roig, and M. Sawicka, Phys. Rev. Lett. **93**, 142503 (2004).

[23] J. Bleck, R. Butt, K. H. Lindenberger, W. Ribbe, and W. Zeitz, Nucl. Phys. A **197**, 620 (1972).

[24] T. Thomas, K. Nomura, V. Werner, T. Ahn, N. Cooper, H. Duckwitz, M. Hinton, G. Ilie, J. Jolie, P. Petkov, and D. Radeck, Phys. Rev. C **88**, 044305 (2013).

[25] T. Thomas, V. Werner, J. Jolie, K. Nomura, T. Ahn, N. Cooper, H. Duckwitz, A. Fitzler, C. Fransen, A. Gade, M. Hinton, G. Ilie, K. Jessen, A. Linnemann, A. Petkov, N. Pietralla, and D. Radeck, Nucl. Phys. A **947**, 203 (2016).

[26] M. Sambataro and G. Mólnar, Nucl. Phys. A **376**, 201 (1982).

[27] F. Iachello and A. Arima, Phys. Lett. B **53**, 309 (1974); Phys. Rev. Lett. **35**, 1069 (1975).

[28] P. D. Duval and R. Barrett, Phys. Lett. B **100**, 223 (1981).

[29] F. Iachello and O. Scholten, Phys. Rev. Lett. **43**, 679 (1979).

[30] F. Iachello and P. van Isacker, *The Interacting Boson-Fermion Model*, Cambridge Monographs on Mathematical Physics (Cambridge University Press, Cambridge, 1991).

[31] B. Pritychenko, M. Birch, B. Singh, and M. Horoi, At. Data Nucl. Data Tables **107**, 1 (2016).

[32] B. Singh, Nucl. Data Sheets **109**, 297 (2008).

[33] O. Scholten, computer codes ODDA and PBEM, KVI Internal Report no. 252, 1982; computer code SPEC (unpublished).

[34] B. S. Reehal and R. A. Sorensen, Phys. Rev. C **2**, 819 (1970).

[35] P. K. Bindal, D. H. Youngblood, R. L. Kozub, and P. H. Hoffmannn-Pinther, Phys. Rev. C **12**, 1826 (1975).

[36] F. Boulay, G. S. Simpson, Y. Ichikawa, S. Kisyov, D. Bucurescu, A. Takamine, D. S. Ahn, K. Asahi, H. Baba, D. L. Balabanski, T. Egami, T. Fujita, N. Fukuda, C. Funayama, T. Furukawa, G. Georgiev, A. Gladkov, M. Hass, K. Imamura, N. Inabe *et al.* Phys. Rev. Lett. **124**, 112501 (2020).

[37] ENSDF - Evaluated Nuclear Structure Data Files, as evaluated and updated by the Brookhaven National Laboratory, https://www.nndc.bnl.gov/ensdf/.

[38] P. Spagnoletti, G. Simpson, S. Kisyov, D. Bucurescu, J. M. Regis, N. Saed-Samii, A. Blanc, M. Jentschel, U. Koster, P. Mutti, T. Soldner, G. deFrance, C. A. Ur, W. Urban, A. M. Bruce, C. Bernards, F. Drouet, L. M. Fraile, L. P. Gaffney, D. G. Ghita *et al.*, Phys. Rev. C **100**, 014311 (2019).

[39] S. Kisyov, D. Bucurescu, J. Jolie, and S. Lalkovski, Phys. Rev. C **93**, 044308 (2016).

[40] D. Bucurescu, Y. Eisermann, G. Graw, R. Hertenberger, H.-F. Wirth, and Yu. V. Ponomarev, Nucl. Phys. A **756**, 54 (2005).

[41] I. S. Towner, Phys. Rep. **155**, 263 (1987).

[42] B. A. Brown, Prog. Part. Nucl. Phys. **47**, 517 (2001).

[43] M. Honma, T. Otsuka, B. A. Brown, and T. Mizusaki, Phys. Rev. C **69**, 034335 (2004).

[44] M. Honma, T. Otsuka, T. Mizusaki, and M. Hjorth-Jensen, Phys. Rev. C **80**, 064323 (2009).

[45] G. Georgiev, I. Matea, D. L. Balabanski, J. M. Daugas, F. de Oliveira Santos, S. Franchoo, F. Ibrahim, F. Le Blanc, M. Lewitowicz, G. Lo Bianco, S. Lukyanov, V. Meot, P. Morel, G. Neyens, Yu. E. Penionzhkevich, A. SaltarellI, O. Sorlin, M. Stanoiu, M. Tarisien, N. Vermeulen, D. Verney, and D. Yordanov, Eur. Phys. J. A **30**, 351 (2006).

[46] B. J. Coombes, A. E. Stuchbery, A. Blazhev, H. Grawe, M. W. Reed, A. Akber, J. T. H. Dowie, M. S. M. Gerathy, T. J. Gray, T. Kibedi, A. J. Mitchell, and T. Palazzo, Phys. Rev. C **100**, 024322 (2019).

[47] R. D. Lawson, *Theory of the Nuclear Shell Model* (Oxford University Press, New York, 1980).